Numerical Heat Transfer, Part B, vol. 18, pp. 61–80, 1990

COMPARATIVE STUDY OF WEIGHTED UPWIND AND SECOND ORDER UPWIND DIFFERENCE SCHEMES

Yousef H. Zurigat and Afshin J. Ghajar
School of Mechanical and Aerospace Engineering, Oklahoma State University, Stillwater, Oklahoma 74078

An extensive survey of difference schemes for approximating the advection terms in the conservation equations of fluid flow and heat transfer was conducted. In this study, two of these schemes, the weighted upwind and the second-order upwind difference schemes (WUDS and SOUDS, respectively), were tested by application to four problems, two of which have not previously been used. The problems involve two-dimensional forced and mixed convection and the predictions were compared with experimental data and/or analytical solutions. The results concur with previous findings and indicate that the SOUDS produces less numerical diffusion than the WUDS and gives predictions in closer agreement with the analytical or experimental data.

INTRODUCTION

Predictions of fluid flow and heat transfer using finite-difference methods are seriously affected by numerical diffusion, instability, and computational cost. Therefore, the choice of the numerical procedure and the discretization scheme are critical to the success and validity of the results.

Many computer codes at present employ discretization schemes based on conventional upwind or donor cell differencing of convective terms. This gives rise to a discretization error (called numerical diffusion) that limits the accuracy and usefulness of predictions. Numerical diffusion has been shown [1] to be significant compared to the physical diffusion. Therefore, it is desirable to reduce these errors so as to enable computer codes to be used as design tools.

The upwind scheme gained popularity among computational fluid practitioners because it is superior to the central difference scheme when the local grid Péclet number is large [2]. However, it was soon recognized that the stability furnished by the upwind scheme was achieved at the expense of accuracy. As a result, thermal hydraulic computer predictions generally produce higher levels of diffusion and mixing than are seen experimentally. Therefore, numerical diffusion is often found to dominate the effects of turbulent diffusion. Hence, turbulence modeling will be overshadowed without the removal of numerical diffusion.

Yousef H. Zurigat's present address is ESM Department, Virginia Polytechnic Institute and State University, Blacksburg, Virginia 24061.

Support for this research provided by the Oklahoma State University Center for Energy Research under grant no. 1150726 and the National Science Foundation under grant no. CBT-88103342 is gratefully acknowledged.

NOMENCLATURE

C_p	specific heat at constant pressure
g	acceleration of gravity
H	effective height between flow inlet and outlet
k	molecular thermal conductivity
l	length scale
P	pressure
Pe	grid Péclet number ($= u^*l/\Gamma$)
Pr	Prandtl number ($= \mu C_p/k$)
r	radius
t	time
t^*	dimensionless time ($= Vt/H$)
T	temperature
u	velocity in the x or r direction
u^*	characteristic velocity
v	velocity in the y direction
V	average vertical velocity
W	tank width
x, y	Cartesian or cylindrical ($x \equiv r$) coordinates
α	donor cell parameter
β	coefficient of thermal expansion $\{= (\rho_0 - \rho)/[\rho_0(T - T_0)]\}$
Γ	diffusion coefficient
ζ	index for Cartesian ($\zeta = 0$) or cylindrical ($\zeta = 1$) coordinate
θ	flow direction angle
μ	absolute viscosity
ρ	density
ϕ	scalar-dependent variable (e.g., P or T)

Subscripts

E	east
i, j	indices of computational grid location
in	at the inlet or inflow
0	initial reference state
u	of the u cell
W	west

Superscripts

T	of the T cell
P	of the P cell
v	of the v cell
u	of the u cell

SURVEY OF DIFFERENCE SCHEMES

The increasing demand for accuracy in numerical computations has led to the development of several new schemes (see Table 1). A number of comparative studies of these schemes has been conducted by application to flow situations with well-established analytical or numerical solutions or with experimental data. Table 2 summarizes the performance of different schemes applied to the flow problems listed in Table 3.

Table 1 Partial List of Discretization Schemes Devised by Various Investigators

No.	Numerical scheme	Contributor
1	Central difference	
2	Upstream (upwind) difference	
3	Hybrid (central and upwind)	Spalding [2]
4	Weighted upwind difference	Hirt et al. [3]
5	Skew upwind difference	Raithby [4]
6	Skew upwind weighted difference	Raithby [4]
7	Quadratic upwind interpolation	Leonard [5]
8	Locally analytical differencing	Wong and Raithby [6]
9	Power-law difference	Patankar [7]
10	Selective grid refinement approach	McGuirk et al. [8]
11	Donor cell corrective scheme	Huh et al. [1]
12	Second-order upwind differencing	Shyy [9]
13	Modified central difference scheme with controlled numerical diffusion	Runchal [10]

Table 2 Comparative Studies of Performance of Various Discretization Schemes from Table 1 as Applied to Various Fluid Flow Problems from Table 3

Contributor	Discretization schemes (Table 1) (numbers in parentheses refer to problems from Table 3)	Main findings reported by the contributor
Runchal [11]	1, 2, 3, (1)	3 is the best from convergence and accuracy points of view.
Raithby [4]	1, 2, 4, 5, 6, (1)	5 and 6 reduce the error greatly, no stability problems.
	2, 5, 6, (2)	Results with 5 and 6 are angle dependent but generally better than 2. Overshoot and undershoot may occur with 5 and 6. Number of iterations for 5 and 6 is larger.
	2, 5, (3)	5 gave much better predictions.
Smith and Hutton [12]	1, 2, 3, 4, 5, 7, 9, (11)	No single scheme emerged as the best.
McGuirk et al. [8]	10, (19)	Grid-independent solution can be obtained using this method.
Claus et al. [13]	5, 5*[a], 7, (2)	Solution is angle dependent. For θ up to 15°, 7 is superior. For $\theta > 15°$, 5 and 5* are superior.
	3, 5*, 7, (4)	7 is superior to 3 and 5*. It responds to grid refinement. 3 and 5* are highly inaccurate.
	3, 5*, 7, (20)	At $\theta = 40°$, 5* and 7 are more accurate than 3. At $\theta = 25°$, 5* is better than 7. 7 displays unphysical oscillations. It is also slower to converge. At $\theta = 0$, all schemes are good.
Syed and Chiappetta [14]	3, 5*, 7, (6)	5* and 7 perform equally well and they are superior to 3. 7 is less sensitive to grid refinement.
	3, 5*, 7, (7)	7 is unstable with fine mesh (uncompatible with TEACH solver).
	3, 5*, 7, (12)	5* is the best.
	3, 5*, 7, (13)	In the initial region with coarse grid the results do not agree with data regardless of the scheme used. With fine grid 7 was excluded. 3 and 5* are comparable.
	3, 5*, 7, (14)	7 is more accurate than 3 and 5*.
	3, 5*, 7, (15)	5* reduces numerical diffusion considerably but there is a disagreement with experiments.

(Table continues on next page)

Table 2 (continued)

Contributor	Discretization schemes (Table 1) (numbers in parentheses refer to problems from Table 3)	Main findings reported by the contributor
Huang et al. [15]	5, 7, 8, 9, (1)	5, 7, and 8 are much better than 9, with 7 being the worst among the best.
	5, 7, 8, 9, (2)	9 gives maximum false diffusion for $\theta = 45°$, 5 gives exact solution. 7 and 8 are superior to 9 but they suffer from overshoots and undershoots. For other flow angles 5 gives rise to more serious overshoots than 7 and 8.
	5, 7, 8, 9, (4)	7 performs exceptionally well. 5 performs poorly, 8 fails to converge.
	5, 7, 8, 9, (16)	At $Pe \simeq 5$, 7 is superior. At low Raleigh number, differences between the schemes were minor.
	5, 7, 8, 9, (17)	Predictions of 5 and 7 in regions of steep velocity gradients are much closer to the true behavior than those of 8 and 9. However, 5 produces oscillations in velocity.
	5, 7, 8, 9, (18)	All schemes but 5 gave excellent agreement. 5 and 9 fail to conserve total pressure.
Runchal et al. [16]	3, 13, (1, 2, 5, 6, 7, 8, 9, 10, 11)	13 is much better in all the cases except in case 5 where the hydrodynamic results were better than 3 but the temperature results were less accurate than 3.
Sharif and Busnaina [17]	4, 5, 7, 12, (2)	4 produces maximum numerical diffusion. For all Péclet numbers 5, 7, and 12 produce less numerical diffusion and have a comparable accuracy. At $\theta = 45°$, 5 is the best. 7 and 12 produce overshoots with the maximum occurring at $\theta = 26.6°$.
	4, 5, 7, 12, (13)	For $\theta = 26.6°$, 5 introduces the least numerical diffusion but exhibits significant oscillation for $\lvert Pe \rvert = \infty$. 4 has the most numerical diffusion. 12 introduces moderate numerical diffusion and oscillation. For $\theta = 45°$, 7 introduces significant oscillations.

[a] 5* is a bounded version of 5.

As shown in Table 2, the results reported by different investigators show that the performance of different schemes is problem dependent. For example, the predictions with the skew upwind difference schemes (SUDS; schemes 5 and 6 of Table 1) are dependent on the angle the flow makes with the grid lines but they both produce low levels of numerical diffusion [4]. However, they may produce overshoots and undershoots

[4, 17]. On the other hand, while the locally analytical differencing scheme performs well when applied to problem 1 (see Table 3), it fails to converge when applied to problem 4 [15]. However, most of the studies cited in Table 2 suggest that the second-order upwind difference scheme (SOUDS), the SUDS, and the quadratic upwind interpolation difference scheme (QUIDS) offer better accuracy than the upwind difference scheme or its derivative, the weighted upwind difference scheme (WUDS).

Further testing of two of the schemes is presented here, with extension of the work to convection flows in Cartesian and cylindrical coordinates. These comparisons were conducted in laminar flow—a convenient test ground. The SOUDS and the WUDS were implemented to solve two-dimensional mixed convection flow problems and the predictions were compared with analytical solutions and/or experimental data. Results concur generally with previous recommendations and the SOUDS scheme was found to be superior in the flows investigated.

Table 3 Fluid Flow Problems Tested by Different Finite-Difference Discretization Schemes

No.	Test problem	Available solution
1	Fluid in a steady state of solid body rotation closed form	
2	Transport of a step change in scalar in a two-dimensional uniform velocity field at an angle	Closed form
3	Interaction of two parallel two-dimensional slot jets	Experimental
4	Square cavity with a moving wall	Numerical (very fine grid)
5	Square cavity with a moving heated wall	Numerical (very fine grid)
6	Laminar flow over a backward facing step	Experimental
7	Turbulent flow over a backward facing step	Experimental
8	Uniform constant velocity flow in straight pipe with exponential temperature distribution	Closed form
9	Same as 8 above with spatially varying heat source	Closed form
10	Recirculating flow with temperature source in a prescribed recirculating velocity field in a square cavity	Closed form
11	Step-like discontinuity in a recirculating flow	Numerical (very fine grid)
12	Swirling flow downstream of a sudden expansion (laminar)	None (reference is made to turbulent experiments)
13	Coannular nonswirling turbulent flow	Experimental
14	Coannular swirling turbulent flow	Experimental
15	Cross-flow multiple jets in duct (three-dimensional)	Experimental
16	Laminar buoyancy-driven cavity flow	Numerical (best available)
17	Laminar impinging jet	None
18	Irrotational corner flow	Closed form
19	Flow downstream of a confined axisymmetric baffle	Experimental
20	Laminar flow with various inlet flow angles	None

MATHEMATICAL MODEL

The flow is governed by the well-known conservation equations of mass, momentum, and energy. It is assumed that the flow is two-dimensional and laminar and that the viscous dissipation is negligible. Also the Boussinesq approximation is invoked; that is, the density is assumed constant except in the buoyancy term of the momentum equations. Then, the governing equations written in primitive variables and in conservative form in both Cartesian ($\zeta = 0$) and cylindrical coordinates ($\zeta = 1$, $x \equiv r$) reduce to:

Continuity:

$$\frac{\partial u}{\partial x} + \frac{\partial v}{\partial y} + \zeta \frac{u}{x} = 0 \tag{1}$$

u and v Momentum:

$$\frac{\partial u}{\partial t} + \frac{\partial uu}{\partial x} + \frac{\partial uv}{\partial y} + \zeta \frac{u^2}{x} = -\frac{1}{\rho_0}\frac{\partial P}{\partial x} + \frac{\partial}{\partial x}\left(\frac{\mu}{\rho_0}\frac{\partial u}{\partial x}\right) + \frac{\partial}{\partial y}\left(\frac{\mu}{\rho_0}\frac{\partial u}{\partial y}\right) + \zeta\left[\frac{\mu}{x\rho_0}\left(\frac{\partial u}{\partial x} - \frac{u}{x}\right)\right] \tag{2}$$

$$\frac{\partial v}{\partial t} + \frac{\partial uv}{\partial x} + \frac{\partial vv}{\partial y} + \zeta \frac{uv}{x} = -\frac{1}{\rho_0}\frac{\partial P}{\partial y} + g_y\,\beta(T - T_0) + \frac{\partial}{\partial x}\left(\frac{\mu}{\rho_0}\frac{\partial v}{\partial x}\right) + \frac{\partial}{\partial y}\left(\frac{\mu}{\rho_0}\frac{\partial v}{\partial y}\right) + \zeta\frac{\mu}{x\rho_0}\frac{\partial v}{\partial x} \tag{3}$$

Energy:

$$\frac{\partial T}{\partial t} + \frac{\partial uT}{\partial x} + \frac{\partial vT}{\partial y} + \frac{\zeta}{x}uT = \frac{\partial}{\partial x}\left(\frac{k}{\rho_0 C_P}\frac{\partial T}{\partial x}\right) + \frac{\partial}{\partial y}\left(\frac{k}{\rho_0 C_P}\frac{\partial T}{\partial y}\right) + \zeta\frac{k}{x\rho_0 C_P}\frac{\partial T}{\partial x} \tag{4}$$

SOLUTION PROCEDURE

The two-dimensional plane or axisymmetric flow domain is divided into rectangular cell divisions, with nonuniform spacing (see Fig. 1). The location of the field variables P, u, v, and T are shown for an arbitrary i,j cell. It is seen that P and T are cell centered while the u and v velocities are located on the faces of the cell. This staggered arrangement eliminates the need for boundary conditions on pressure and allows for ease in setting the boundary conditions on velocities. A layer of fictitious cells is added on all sides of the computational domain to facilitate the application of momentum and thermal boundary conditions. The staggered arrangement described above gives rise to three different control

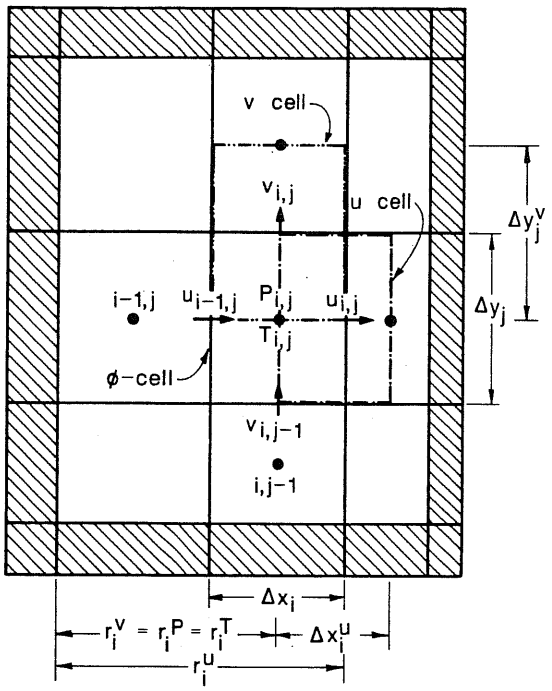

Fig. 1 Grid layout showing location of the nodal variables u, v, P, and T, ij notation, and the ϕ (T, P), u, and v cells.

volumes: the u cell, the v cell, and the ϕ cell for solving the x (or r) momentum, the y momentum, and the scalar transport equations, respectively (see Fig. 1).

Approximation of the advection terms requires special treatment that has been the topic of numerous studies. The explicit formulation of Sharif and Busnaina [17] for discretizing the conservation equations in Cartesian coordinates is adopted and extended to axisymmetric cylindrical coordinates. Standard differencing techniques of Hirt et al. [3] are used except for the advection terms, which are approximated differently for the WUDS and SOUDS methods (see [17, 18]). To illustrate the difference between the two methods, the finite-difference discretization expressions for the advection term $(\partial uu/\partial x)_{i,j}$ in Eq. (2) are presented in the appendix at the end of the paper.

In examining Eqs. (1)–(4), two observations are in order:

1. The presence of temperature-dependent source term: the buoyancy term in Eq. (3) results in coupling between velocity and temperature (i.e., momentum-to-energy coupling). On the other hand, velocities appearing in the advection terms in the energy equation [Eq. (4)] result in the converse energy-to-momentum coupling. This bidirectional coupling generally requires an iterative solution. However, the explicit formulation described above requires a small time step, which results in small temperature changes and buoyancy forces thereafter.
2. The absence of a separate equation for pressure poses a problem in calculating the flow field variables. The pressure appears in both the u and v momentum equations. This velocity-pressure coupling requires special treatment since the accuracy of the computed pressure field determines that of the computer velocity field, which in turn determines the satisfaction of continuity requirements. Thus

for a given initial guess of the pressure field or for that calculated from a previous time step, the calculated velocity field will not, in general, satisfy the continuity equation. An iterative adjustment of the cell-centered pressure and the cell-boundary velocities at each computational cell is employed, sweeping over the computational domain repeatedly until the absolute value of the residual calculated from the continuity equation at each cell becomes vanishingly small, within a prescribed tolerance. General and special boundary conditions are applied at the beginning of each iteration of the above procedure (see [3]).

RESULTS AND DISCUSSION

The computer code that was developed based on the procedure described above was tested by application first to simple flow problems and then to two-dimensional mixed convection problems.

Uniform Flow with a Step Change in Temperature

Consider the plug flow situation with a constant velocity and a sudden change in temperature at the inlet. The flow is considered to be one-dimensional and only a few terms in the governing energy equation are retained while the velocity v is constant and $u = 0$. This problem has been widely used as a test problem to investigate the numerical diffusion resulting from the application of different numerical schemes. In this case, however, the cross-flow diffusion is absent, leaving only the truncation error diffusion added to the physical diffusion.

The stability and accuracy of the WUDS requires a certain amount of upstream differencing to maintain both stability and a low level of numerical diffusion (donor cell parameter α). Figure 2 shows the transient response to a step change in temperature for different values of α. The temperature is monitored at $y/H = 0.3417$. Oscillations are persistent even for $\alpha = 0.35$, which falls within the range $1 > \alpha > \max[u\Delta t/\Delta x, v\Delta t/\Delta y]$, the criterion given by Hirt et al. [3], the lower range being 0.15. This indicates that the mentioned criterion is not universal and the value of α that produces an oscillation-free solution should be chosen by testing. For $\alpha = 0.5$, no oscillations are present.

When solving the same problem using SOUDS, the solution, while being stable, exhibits undershoot (see Fig. 3). To suppress the undershoot and/or overshoots, a simple procedure known as "bounding" [17] produces a wiggles-free solution as shown in Fig. 3. In this bounding procedure, the calculated value for a particular cell is compared to the calculated values of its surrounding cells and reset as follows:

$$\phi_{i,j} = \begin{cases} \phi_{\max} & \text{if } \phi_{i,j} > \phi_{\max} \\ \phi_{i,j} & \text{if } \phi_{\min} < \phi_{i,j} < \phi_{\max} \\ \phi_{\min} & \text{if } \phi_{i,j} < \phi_{\min} \end{cases} \tag{5}$$

where

$$\phi_{\max} = \max\{\phi_{i-1,j}, \phi_{i+1,j}, \phi_{i,j-1}, \phi_{i,j+1}\} \tag{6}$$

$$\phi_{\min} = \min\{\phi_{i-1,j}, \phi_{i+1,j}, \phi_{i,j-1}, \phi_{i,j+1}\} \tag{7}$$

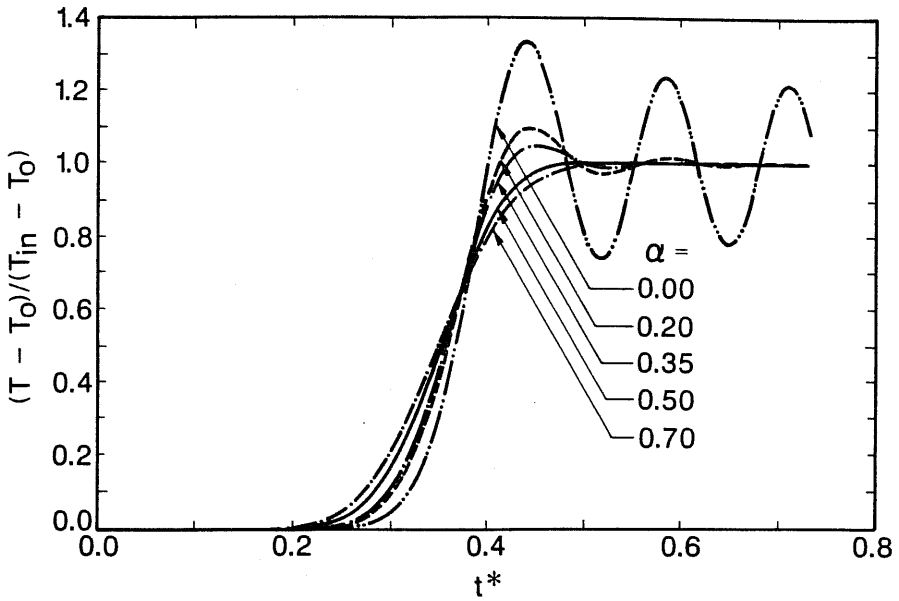

Fig. 2 Transient response to a step change in temperature in plug flow (cylindrical) using WUDS with different values of upstream differencing parameter α.

Figure 4 compares the solutions shown in Figs. 2 and 3 and the analytical solution. It is seen that the SOUDS introduces less numerical diffusion as compared with WUDS ($\alpha = 0.5$). Note that in these calculations Pe = 422, grid size = 1.83 cm × 0.91 cm, time step = 0.2 s, and Pr = 5.55.

Uniform Flow at 45° to the Grid Lines with a Step Change in Temperature

Consider the flow situation shown in Fig. 5. Two streams at uniform known identical velocities, but different temperatures, cut through the computational domain at 45°. This is another test problem widely used in computational fluid dynamics since both the truncation and cross-flow diffusion are present.

Figure 6 shows the temperature profile monitored at the diagonal of the flow domain. It can be seen that the SOUDS, while exhibiting overshoots and undershoots, substantially reduces the numerical diffusion as compared with WUDS. The exact solution shown in Fig. 6 is an inviscid solution.

Mixed Convection Flow

Consider the problem of transient mixed convection flow in a thermal storage tank shown in Fig. 7. The transient temperature profiles along the height of the tank were monitored at $x/W = 0.5$. The solutions generated using WUDS and SOUDS are compared to the predictions obtained by Chan et al. [19] who used WUDS with primitive variables and the same grid configuration (see Fig. 8). In these calculations, Pe >> 2, grid size = 3.56 cm × 3.56 cm, and time step = 2 s. A close agreement is seen to exist between the present WUDS predictions and those of Chan et al. [19]. Moreover, the predictions

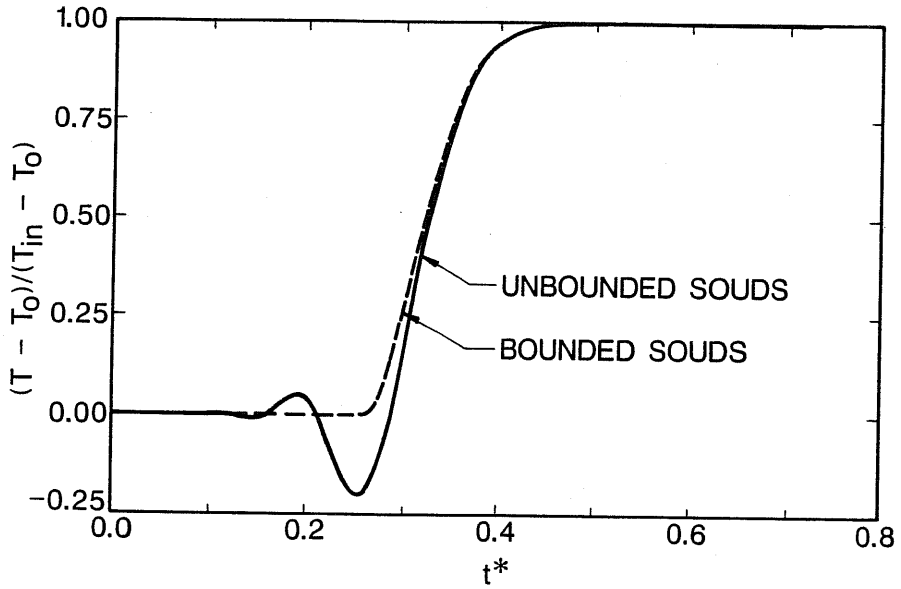

Fig. 3 Transient response to a step change in temperature in plug flow (cylindrical) using SOUDS with and without bounding.

of the SOUDS seem, in general, to exhibit less total diffusion, which implies less numerical diffusion. The computer time for both methods is comparable, with SOUDS converging slightly faster.

As mentioned earlier, the results of Chan et al. [19] were obtained using WUDS. The slight disagreement between the present and published results could be due to several

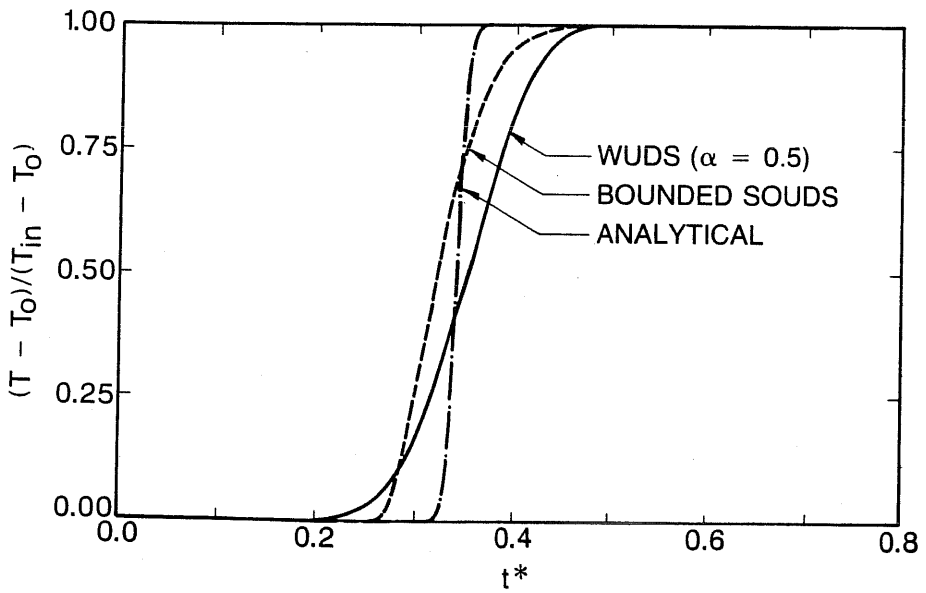

Fig. 4 Comparison of bounded SOUDS and WUDS with the analytical solution for the case of Figs. 2 and 3.

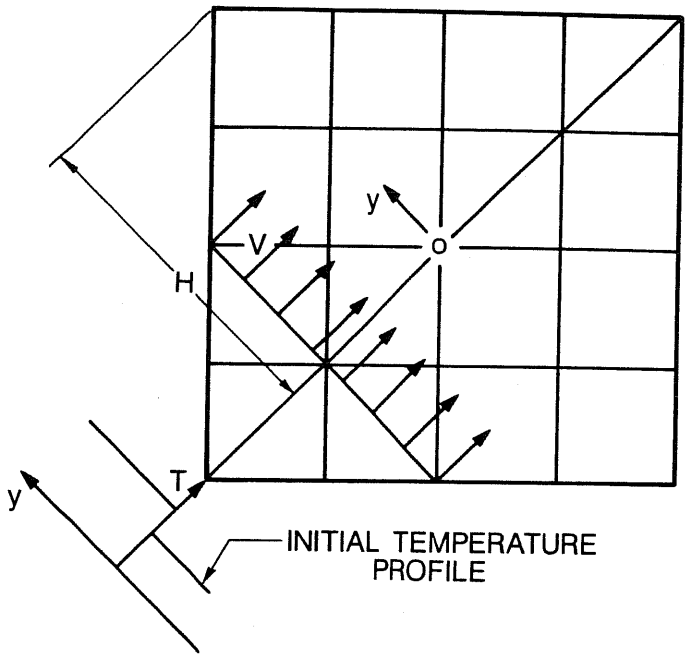

Fig. 5 Uniform flow at 45° to the grid lines with a step change in temperature.

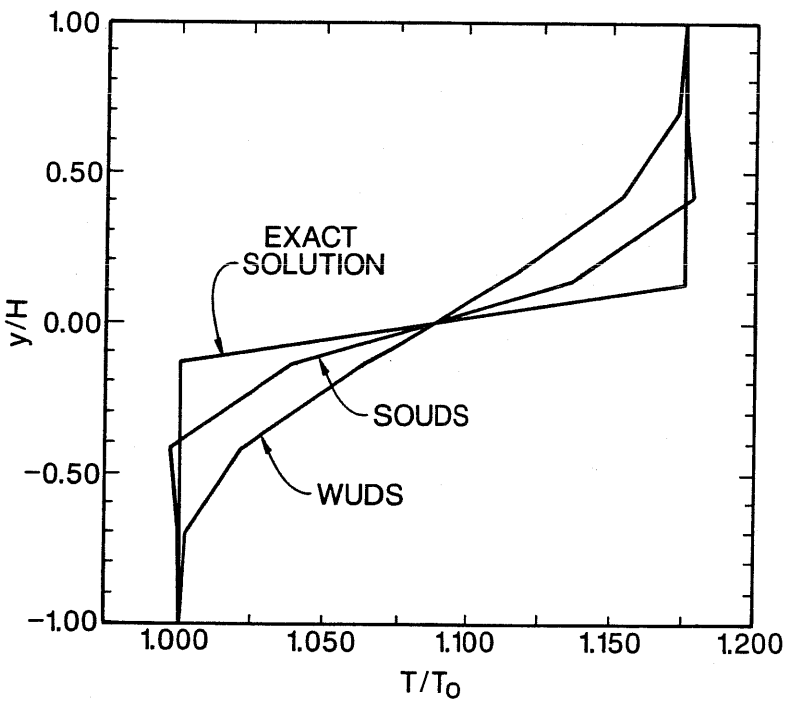

Fig. 6 Temperature profiles of two interacting parallel streams shown in Fig. 5 as calculated with WUDS and SOUDS.

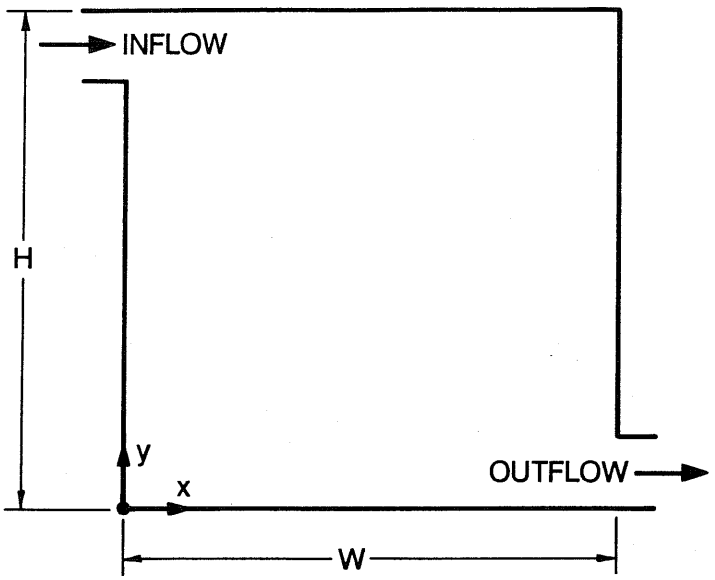

Fig. 7 System geometry for transient mixed convection flow problem [19].

reasons, for example, the choice of donor cell parameter α, the time step, the initialization of the velocity field, and the convergence tolerance employed. All these factors affect the solution obtained with WUDS.

The bounding of SOUDS does not seem to affect the solution greatly. Figure 9 shows the solutions with and without bounding. The undershoot, although small, is quite

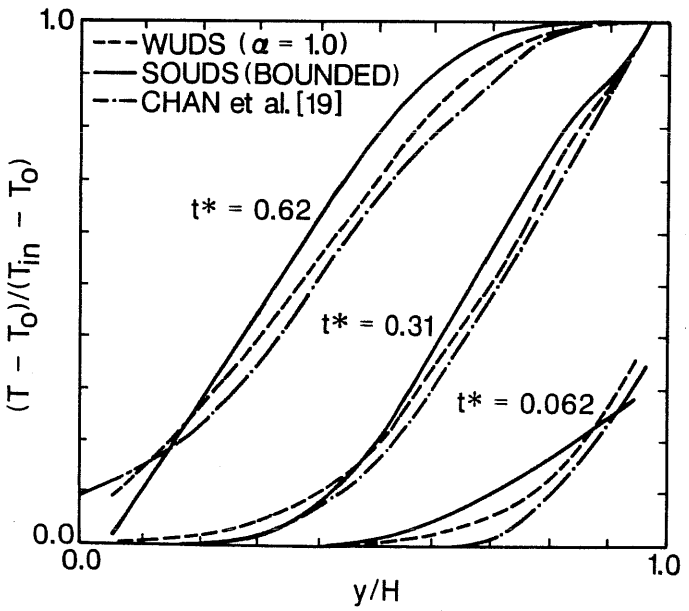

Fig. 8 Predicted transient temperature profiles in thermal storage tank using WUDS (α = 1.0) and SOUDS compared with results of [19] at x/W = 0.5.

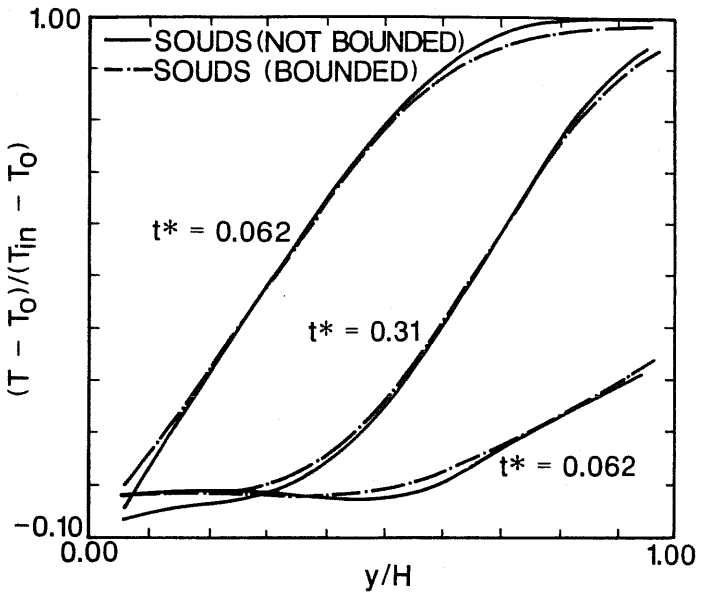

Fig. 9 Comparison of bounded and unbounded SOUDS predictions of transient temperature profiles of mixed convection flow problem at $x/W = 0.5$.

clear. The dashed curves represent the solution shown in Fig. 8 with the scale being slightly altered. The difference, excluding the undershoots, is not significant.

Application of the two methods to thermocline thermal storage [20] shows that the performance of SOUDS is much better than WUDS. Figure 10 shows the predictions compared with the experiment. The agreement between the predictions using SOUDS and the experiment is satisfactory. A high level of numerical diffusion is seen when using WUDS. Figure 11 shows the same trend. These calculations were carried out with Pe = 387, grid size = 2.13 cm × 5.77 cm, time step = 0.15 s, and Pr = 4.5.

The results obtained indicate that the choice of the solution scheme is an important factor in achieving realistic predictions. Based on the results discussed in the foregoing, the SOUDS produces results in closer agreement with analytical and experimental data.

CLOSURE

Numerical diffusion resulting from difference approximation of advection terms in the governing equations of fluid flow and heat transfer has been the subject of numerous studies. Several difference schemes were devised by different investigators to reduce numerical diffusion. The literature survey conducted in this study suggests that the SOUDS, SUDS, and QUIDS offer a lower level of numerical diffusion and better accuracy than the conventional upwind difference scheme or its derivative, the WUDS.

Testing of two of these schemes was conducted in this study by application to forced and mixed convection flow problems. The SOUDS and WUDS were implemented in a computer code, which was applied to solve the test problems discussed in the previous section. The results indicate that the SOUDS produces predictions in closer agreement with the analytical and experimental data than the WUDS. This confirms the previous findings in the literature while using some test problems that have not previously been

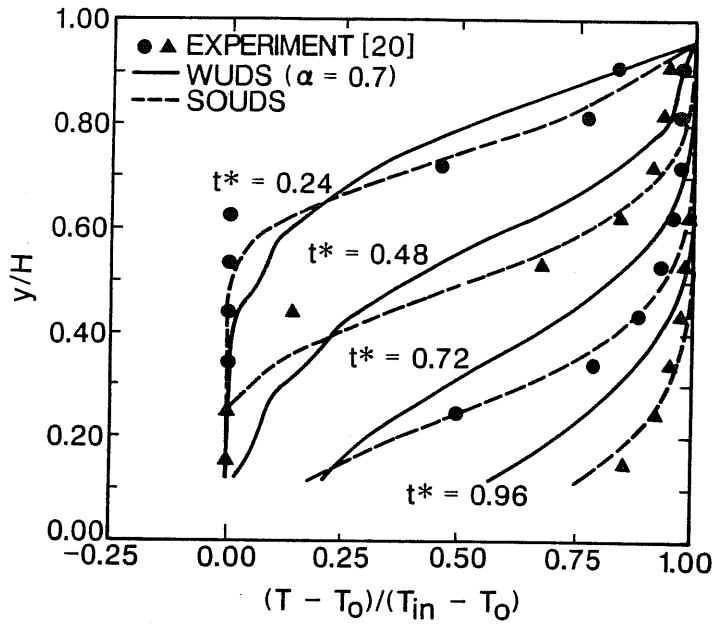

Fig. 10 Predictions of temperature profiles at the centerline in thermocline cylindrical thermal storage tank comparing SOUDS, WUDS (α = 0.7), and the experiments of [20].

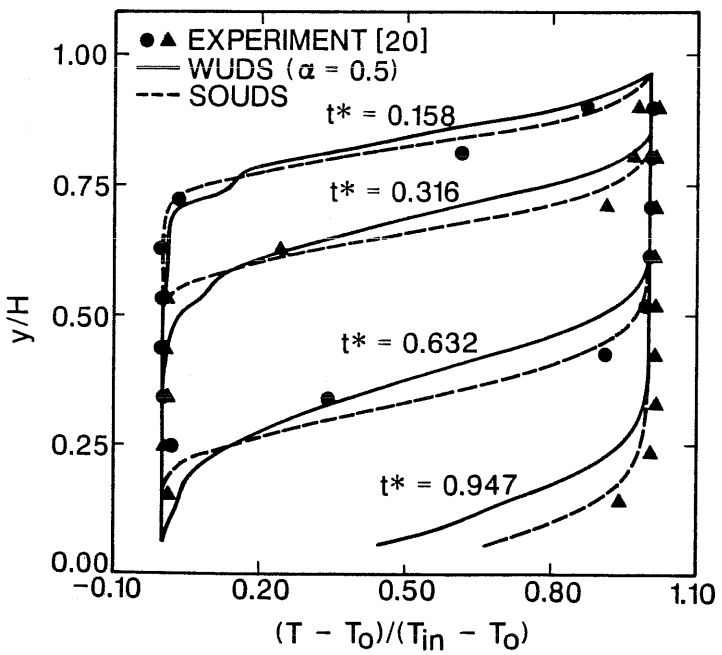

Fig. 11 Predictions of temperature profiles at the centerline in thermocline cylindrical thermal storage tank comparing SOUDS, WUDS (α = 0.5), and the experiments of [20].

used. The advantage of SOUDS over WUDS was clearly demonstrated, indicating that the choice of the difference scheme is critical to the validity of the predictions and design assessments thereafter.

APPENDIX

In this appendix, the discretization expressions for the advection term $(\partial uu/\partial x)_{i,j}$ are derived for both WUDS and SOUDS methods.

WUDS Method

Consider the u cell control volume shown in Fig. A1. The discretization of the advected u velocity can be written as

$$\left(\frac{\partial uu}{\partial x}\right)_{i,j} = \frac{u_{E,u}\tilde{u}_E - u_{W,u}\tilde{u}_W}{\Delta x_i^u} \tag{A1}$$

where $u_{E,u}$ and $u_{W,u}$ are the velocities at the east and west faces of the u cell correspondingly. These are given by

$$u_{E,u} = 0.5(u_{i+1,j} + u_{i,j}) \tag{A2a}$$

$$u_{W,u} = 0.5(u_{i,j} + u_{i-1,j}) \tag{A2b}$$

and $\tilde{u}_E$ and $\tilde{u}_W$ assume different forms depending on the type of discretization considered. For example, in central difference scheme they are given by

$$\tilde{u}_E = u_{E,u} \tag{A3a}$$

$$\tilde{u}_W = u_{W,u} \tag{A3b}$$

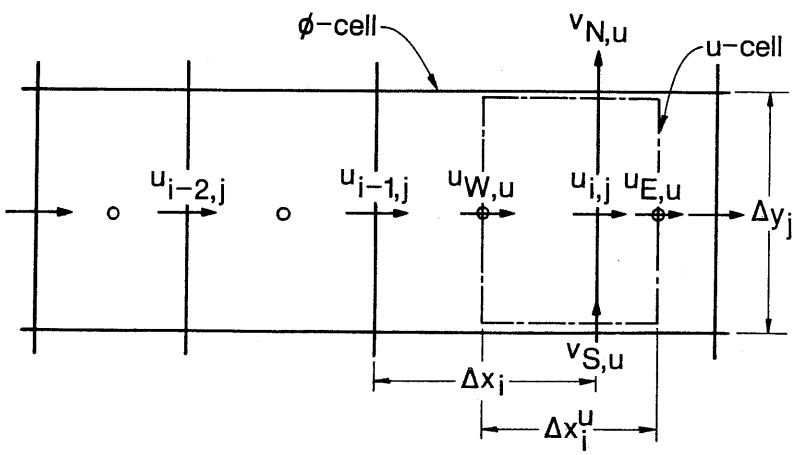

Fig. A1 Grid system showing the u cell and location of related velocities.

which, when substituted in Eq. (A1), give the central difference form

$$\left(\frac{\partial uu}{\partial x}\right)_{i,j} = \frac{(u_{i+1,j} + u_{i,j})^2 - (u_{i,j} + u_{i-1,j})^2}{4\Delta x_i^u} \tag{A4}$$

For a fully upwind scheme the velocities $\bar{u}_E$ and $\bar{u}_W$ are expressed taking into account the flow direction. This is done by analogy with the tank-and-tube model [7]. For $u > 0$ we have

$$\bar{u}_E = u_{i,j} \tag{A5a}$$

$$\bar{u}_W = u_{i-1,j} \tag{A5b}$$

and for $u < 0$

$$\bar{u}_E = u_{i+1,j} \tag{A5c}$$

$$\bar{u}_W = u_{i,j} \tag{A5d}$$

Substitution of Eqs. (A5) in Eq. (A1) gives the upwind difference form. Thus for $u > 0$ we get

$$\left(\frac{\partial uu}{\partial x}\right)_{i,j} = \frac{(u_{i+1,j} + u_{i,j})u_{i,j} - (u_{i,j} + u_{i-1,j})u_{i-1,j}}{2\Delta x_i^u} \tag{A6}$$

and for $u < 0$ we have

$$\left(\frac{\partial uu}{\partial x}\right)_{i,j} = \frac{(u_{i+1,j} + u_{i,j})u_{i+1,j} - (u_{i,j} + u_{i-1,j})u_{i,j}}{2\Delta x_i^u} \tag{A7}$$

The WUDS is obtained by combining Eqs. (A4), (A6), and (A7) using a donor cell parameter α, which assumes values between zero and unity [3]:

$$\left(\frac{\partial uu}{\partial x}\right)_{i,j} = [(u_{i,j} + u_{i+1,j})^2 + \alpha|u_{i,j} + u_{i+1,j}|(u_{i,j} - u_{i+1,j}) - (u_{i-1,j} + u_{i,j})^2 - \alpha|u_{i-1,j} + u_{i,j}|(u_{i-1,j} - u_{i,j})]/4\Delta x_i^u \tag{A8}$$

Equation (A8) reduces to Eq. (A4) for $\alpha = 0.0$, to Eq. (A6) for $\alpha = 1.0$ and $u > 0$, and to Eq. (A7) for $\alpha = 1.0$ and $u < 0$. Sharif and Busnaina [17] have expressed $\bar{u}_E$ and $\bar{u}_W$ in a form more suitable for implementation in a computer code. That is,

$$\bar{u}_E = 0.5[u_{i,j} + u_{i+1,j} + (is)\alpha(u_{i,j} - u_{i+1,j})] \tag{A9}$$

where $is = u_{E,u}/|u_{E,u}|$, and $u_{E,u}$ is given by Eq. (A2a).

$$\tilde{u}_W = 0.5[u_{i-1,j} + u_{i,j} + (is)\alpha(u_{i-1,j} - u_{i,j})] \tag{A10}$$

where $is = u_{W,u}/|u_{W,u}|$ and $u_{W,u}$ is given by Eq. (A2b).

SOUDS Method

For the SOUDS method the discretization of the advected u velocity is also given by Eq. (A1). The velocities $\tilde{u}_E$ and $\tilde{u}_W$ appearing in the equation are derived as follows.

Depending on the flow direction, the velocities $\tilde{u}_E$ and $\tilde{u}_W$ are expressed in terms of velocities upstream of the location of interest. For example, for $u > 0$, $\tilde{u}_E$ is expressed in terms of $u_{i,j}$ and $u_{i-1,j}$, and similarly, $\tilde{u}_W$ is expressed in terms of $u_{i-1,j}$ and $u_{i-2,j}$. Thus, extrapolation for $\tilde{u}_E$ from $u_{i,j}$ and $u_{i-1,j}$ gives, for $u > 0$,

$$\tilde{u}_E = \frac{(2\Delta x_i + \Delta x_{i+1})u_{i,j} - \Delta x_{i+1}u_{i-1,j}}{2\Delta x_i} \tag{A11}$$

and for $\tilde{u}_W$ from $u_{i-1,j}$ and $u_{i-2,j}$ gives

$$\tilde{u}_W = \frac{(2\Delta x_{i-1} + \Delta x_i)u_{i-1,j} - \Delta x_i u_{i-2,j}}{2\Delta x_{i-1}} \tag{A12}$$

Equation (A11) can be written as

$$\tilde{u}_E = (1 + r_1)u_{i,j} - r_1 u_{i-1,j} \tag{A13}$$

where $r_1 = \Delta x_{i+1}/2\Delta x_i = \Delta xh_{i+1}/\Delta x_i$, and $\Delta xh_{i+1} = \Delta x_{i+1}/2$.

Similarly for $\tilde{u}_W$ we get

$$\tilde{u}_W = (1 + r_2)u_{i-1,j} - r_2 u_{i-2,j} \tag{A14}$$

where $r_2 = \Delta x_i/2\Delta x_{i-1} = \Delta xh_i/\Delta x_{i-1}$.

When $u < 0$, extrapolation for $\tilde{u}_E$ from $u_{i+1,j}$ and $u_{i+2,j}$ gives

$$\tilde{u}_E = \frac{(2\Delta x_{i+2} + \Delta x_{i+1})u_{i+1,j} - \Delta x_{i+1}u_{i+2,j}}{2\Delta x_{i+2}} \tag{A15}$$

and for $\tilde{u}_W$ from $u_{i,j}$ and $u_{i+1,j}$ gives

$$\tilde{u}_W = \frac{(2\Delta x_{i+1} + \Delta x_i)u_{i,j} - \Delta x_i u_{i+1,j}}{2\Delta x_{i+1}} \tag{A16}$$

These equations can be rewritten as

$$\tilde{u}_E = (1 + r_3)u_{i+1,j} - r_3 u_{i+2,j} \tag{A17}$$

where $r_3 = \Delta x_{i+1}/2\Delta x_{i+2} = \Delta x h_{i+1}/\Delta x_{i+2}$. Similarly for $\tilde{u}_W$ we get

$$\tilde{u}_W = (1 + r_4)u_{i,j} - r_4 u_{i+1,j} \tag{A18}$$

where $r_4 = \Delta x_i/2\Delta x_{i+1} = \Delta x h_i/\Delta x_{i+1}$.

Equations (A13) and (A17) for $\tilde{u}_E$ can be combined in one recurrence relation [17] as

$$\tilde{u}_E = (1 + r)u_{i+ia,j} - ru_{i-1+3ia,j} \tag{A19}$$

where $$r = \frac{\Delta x h_{i+1}}{\Delta x_{i+2ia}}$$

$$ia = \frac{1 - is}{2}$$

$$is = \frac{u_{E,u}}{|u_{E,u}|}$$

Note that Eq. (A19) reduces to Eq. (A13) for $u > 0$ and to Eq. (A17) for $u < 0$.

In a similar fashion, Eqs. (A14) and (A18) for $\tilde{u}_W$ are combined in the following relation:

$$\tilde{u}_W = (1 + r)u_{i-1+ia,j} - ru_{i-2+3ia,j} \tag{A20}$$

where $$r = \frac{\Delta x h_i}{\Delta x_{i-1+2ia}}$$

$$ia = \frac{1 - is}{2}$$

$$is = \frac{u_{W,u}}{|u_{W,u}|}$$

REFERENCES

1. K. Y. Huh, M. W. Golay, and V. P. Manno, A Method for Reduction of Numerical Diffusion in the Donor Cell Treatment of Convection, *J. Comput. Phys.*, vol. 63, pp. 201–221, 1986.
2. D. B. Spalding, A Novel Finite Difference Formulation for Differential Expressions Involving Both First and Second Derivatives, *Int. J. Numer. Methods Eng.*, vol. 4, pp. 551–559, 1972.
3. C. W. Hirt, B. D. Nichols, and N. C. Romero, SOLA—A Numerical Solution Algorithm for Transient Fluid Flows, Report No. LA-5852, Los Alamos Scientific Laboratory, Los Alamos, New Mexico, April 1975.

4. G. D. Raithby, Skew-Upstream Differencing Schemes for Problems Involving Fluid Flow, *Comput. Methods Appl. Mech. Eng.*, vol. 9, pp. 153–164, 1976.
5. B. P. Leonard, A Stable and Accurate Convective Modeling Procedure Based on Quadratic Upstream Interpolation, *Comput. Methods Appl. Mech. Eng.*, vol. 19, pp. 59–98, 1979.
6. H. H. Wong and G. D. Raithby, Improved Finite-Difference Methods Based on a Critical Evaluation of the Approximating Errors, *Numer. Heat Transfer*, vol. 2, pp. 139–163, 1979.
7. S. V. Patankar, *Numerical Heat Transfer and Fluid Flow*, Hemisphere, Washington, D.C., 1980.
8. J. J. McGuirk, A. M. K. P. Taylor, and J. H. Whitelaw, The Assessment of Numerical Diffusion in Upwind Difference Calculations of Turbulent Recirculating Flows, in L. J. S. Bradbury et al. (eds.), *Turbulent Shear Flows 3*, Springer-Verlag, New York, pp. 206–224, 1982.
9. W. Shyy, A Study of Finite Difference Approximations to Steady State Convection Dominated Flow Problems, *J. Comput. Phys.*, vol. 57, pp. 415–438, 1985.
10. A. K. Runchal, CONDIF: A Modified Central-Difference Scheme with Unconditional Stability and Very Low Numerical Diffusion, in C. L. Tien et al. (eds.), *Proc. Eighth Int. Heat Transfer Conf.*, San Francisco, Calif., 1986.
11. A. K. Runchal, Convergence and Accuracy of Three Finite Difference Schemes for a Two-Dimensional Conduction and Convection Problem, *Int. J. Numer. Methods in Eng.*, vol. 4, pp. 541–550, 1972.
12. R. M. Smith and A. G. Hutton, The Numerical Treatment of Advection: A Performance Comparison of Current Methods, *Numer. Heat Transfer*, vol. 5, pp. 439–461, 1982.
13. R. W. Claus, G. M. Neely, and S. A. Syed, Reducing Numerical Diffusion for Incompressible Flow Calculations, NASA-TM-83621, 1984.
14. S. Syed and L. Chiappetta, Finite Difference Methods for Reducing Numerical Diffusion in TEACH-Type Calculations, AIAA Paper AIAA-85-0057, AIAA 23rd Aerospace Science Meeting, Reno, Nev., 1985.
15. P. G. Huang, B. E. Launder, and M. A. Leschziner, Discretization of Nonlinear Convection Processes—A Broad-Range Comparison of Four Schemes, *Comput. Methods Appl. Mech. Eng.*, vol. 48, no. 1, pp. 1–24, 1985.
16. A. K. Runchal, M. S. Anand, and C. Mongia, An Unconditionally Stable Central Differencing Scheme for High Reynolds Number Flows, AIAA Paper AIAA-87-0060, AIAA 25th Aerospace Science Meeting, Reno, Nev., 1987.
17. A. R. Sharif and A. A. Busnaina, Assessment of Finite Difference Approximations for the Advection Terms in the Simulation of Practical Flow Problems, *J. Comput. Phys.*, vol. 74, pp. 143–176, 1988.
18. Y. H. Zurigat, An Experimental and Analytical Examination of Stratified Thermal Storage, Ph.D. thesis, Oklahoma State University, Stillwater, Ok., 1988.
19. A. M. C. Chan, P. S. Smereka, and D. Giusti, A Numerical Study of Transient Mixed Convection Flows in a Thermal Storage Tank, *ASME Trans. J. Sol. Eng.*, vol. 105, pp. 246–253, 1983.
20. Y. H. Zurigat, P. R. Liche, and A. J. Ghajar, Influence on Inlet Geometry on Mixing in Thermocline Thermal Energy Storage, *Int. J. Heat and Mass Transfer* (in press).

Received 16 May 1989
Accepted 6 November 1989